

U.S. DEPARTMENT OF THE INTERIOR  
U.S. GEOLOGICAL SURVEY

Rapid computation of electromagnetic fields for high-frequency sounding  
in the 300 kHz to 30 MHz range over layered media

by

Walter L. Anderson \*

Open-File Report 94-196

1994

This report is preliminary and has not been reviewed for conformity with U.S. Geological Survey editorial standards. Use of trade names in this report is for descriptive purposes only and does not necessarily imply endorsement by the USGS.

-----  
\* U.S. Geological Survey, MS 964, Box 25046, Denver, Colorado, 80225

## Introduction

A new method for rapid computation of electromagnetic (EM) fields for high-frequency sounding (HFS) over a layered earth is presented in this report. The essence of the new method uses a Q-factor correction for extending a closed-form half-space analytic solution to a layered earth model. Use of the Q-factor in this context was first studied by Wait (1962; p.53-61). Kraichman (1976) also discusses when the Q-factor method can be used to provide a good approximation to an exact layered earth solution.

According to Wait (1962) and Kraichman (1976), the Q-factor approach may be used if the dipole fields can be approximated by a single normally incident plane wave at the receiver in the top layer. Fortunately, for the high-frequency range of interest with the HFS system, and with moderately conductive and dielectric earth models, the Q-factor method (also called the HFS Q-method) is usually a very good approximation to the exact solution for a layered earth. Examples of computing layered earth responses by the HFS Q-method and exact numerical integration method will be given for comparison of several typical models encountered in shallow HFS studies.

Because the Q-factor method does not require any numerical integrations, the layered earth HFS Q-method algorithm is very fast (even on PCs). In general, the computations only require elementary complex functions, and in one case, modified Bessel functions of a complex argument. (See equations (1)-(3) below.)

## Mathematical Theory for the HFS System

The mathematical theory and system development for the HFS system can be found in Stewart's (1993) PhD thesis, and the references contained therein. A case history paper on use of the HFS in field applications is also given by Stewart et al. (1994). In the latter paper, mention of a quick reconnaissance method of HFS data inversion is given by Anderson (1991), where complex image theory and the Q-factor method was first introduced to obtain fast approximate image solutions for layered models.

To obtain improved forward and/or inverse solutions for HFS over a layered earth, I begin with an exact half-space formulation (Wait, 1954) for the magnetic  $H$  fields and electric  $E$  field components in cylindrical coordinates for a vertical magnetic dipole (VMD) loop source on the earth's surface, with  $\exp(+i\omega t)$  time dependence,

$$H_z = -m[(9+9\gamma_0 r + 4\gamma_0^2 r^2 + \gamma_0^3 r^3)e^{-\gamma_0 r} - (9+9\gamma_1 r + 4\gamma_1^2 r^2 + \gamma_1^3 r^3)e^{-\gamma_1 r}]/[2\pi(\gamma_1^2 - \gamma_0^2)r^5] , \quad (1)$$

$$H_r = -m[-(\gamma_1^2 - \gamma_0^2)I_2(z_1)K_2(z_2) + (\gamma_1^2 + \gamma_0^2)I_1(z_1)K_1(z_2)]/(4\pi r) , \quad (2)$$

$$E_{\varphi} = -i\omega\mu_0 m [(3+3\gamma_0 r + \gamma_0^2 r^2) e^{-\gamma_0 r} - (3+3\gamma_1 r + \gamma_1^2 r^2) e^{-\gamma_1 r}] / [(\gamma_1^2 - \gamma_0^2) r^4], \quad (3)$$

where

$$\begin{aligned} \gamma_0^2 &= -\omega^2 \epsilon_0 \mu_0, \quad \omega = 2\pi f \quad (f > 0 \text{ Hertz}), \\ \gamma_1^2 &= -\omega^2 \epsilon \mu_0 + i\omega \mu_0 \sigma, \quad i = (-1)^{1/2}, \\ \mu_0 &= 4\pi 10^{-7} \text{ H/m}, \quad \epsilon_0 = 8.854 \cdot 10^{-12} \text{ F/m}, \end{aligned} \quad (4)$$

and

$$z_1 = (\gamma_1 - \gamma_0) r / 2, \quad z_2 = (\gamma_1 + \gamma_0) r / 2. \quad (5)$$

In equations (1)-(5),  $r$  is the VMD transmitter and receiver separation, where  $r > 0$  m, and  $m$  is the magnetic dipole moment (ampere-m<sup>2</sup>). The terms  $I_n(z)$  and  $K_n(z)$  in equation (2) are modified Bessel functions of order  $n$  and complex argument  $z$  defined in equation (5).

In general, the propagation terms ( $\gamma_0$  in air,  $\gamma_1$  in earth) in equations (4) can have the electrical conductivity ( $\sigma$ ), magnetic permeability ( $\mu$ ), and dielectric permittivity ( $\epsilon$ ) vary as a function of angular frequency ( $\omega$ ). In addition, each of these parameters can also be complex. However, in this report, I will only consider the special case where each of the material parameters ( $\sigma$ ,  $\mu$ ,  $\epsilon$ ) are real and do not vary with frequency in the earth, or in each layer of an M-layer model. Furthermore, for typical earth models,  $\mu_0$  can be fixed in  $\gamma_1$  in equation (4).

To extend the half-space formulas to account for an M-layered earth with thicknesses  $h_j$  ( $j=1, \dots, M-1$ ) and propagation terms  $\gamma_j$ , a backward recurrence relation can be used to define a Q-factor at the surface,  $Q^{(1)}$ , as follows,

$$\begin{aligned} Q^{(j-1)} &= \frac{\gamma_{j-1} Q^{(j)} + \gamma_j \tanh(\gamma_{j-1} h_{j-1})}{\gamma_j + \gamma_{j-1} Q^{(j)} \tanh(\gamma_{j-1} h_{j-1})}, \\ \tanh(\gamma_{j-1} h_{j-1}) &= \frac{1 - e^{-2\gamma_{j-1} h_{j-1}}}{1 + e^{-2\gamma_{j-1} h_{j-1}}}, \end{aligned} \quad (6)$$

$$\gamma_j^2 = -\omega^2 \epsilon_j \mu_0 + i\omega \mu_0 \sigma_j, \quad j = M, M-1, \dots, 2, \quad Q^{(M)} = 1.$$

Finally, the effect of layering below the air-earth interface is accounted for by simply substituting  $\gamma_1^*$  for  $\gamma_1$  in equations (1)-(5) using the relation,

$$\gamma_1^* = \gamma_1 / Q^{(1)}. \quad (7)$$

It should be noted that the modified Bessel function products for  $H_r$  in equation (2) can be conveniently evaluated in parallel for  $n=1,2$  by applying the useful relationships,

$$I_n(z_1)K_n(z_2) = e^{|x_1|-z_2} [e^{-|x_1|} I_n(z_1)] [e^{z_2} K_n(z_2)] , \quad (8)$$

$$z_1 = x_1 + i y_1, \quad z_2 = x_2 + i y_2.$$

Many Bessel function algorithms can compute the terms in brackets recursively in equation (8) more easily than separate Bessel function terms, and hence, the trick of factoring the exponential terms as shown is a very efficient and accurate method.

### Examples

The examples in this section are selected to show some typical type-curves expected for the USGS prototype HFS hardware over lossy layered earth models. The present HFS range is approximately 300 kHz to 24 MHz, however the examples given below have an expanded frequency range to purposely illustrate the behavior of sounding curves outside this range.

The forward sounding curves in Figure 1 show comparisons between three different methods of computation. The response functions displayed in Figure 1(a) and (b) are the magnetic field polarization ellipse parameters: tilt angle and ellipticity (Smith and Ward, 1974). As currently used with the HFS hardware (Stewart, 1993), the vertical magnetic source and receiver loops are each elevated at .255 m with a given  $r$ -separation noted in Figure 1(a), where the transmitter loop has a fixed radius of .1524 m. (The same loop geometry is used in all examples below, where selected layered earth parameters are denoted in part b of each figure.)

The HFS Q-method (solid curve) in Figure 1 uses formulas (1)-(5) derived with the Q-factor correction given by equations (6)-(7) for a layered earth. The numerical integration method (dashed curve) uses the formulas from Ryu et al. (1970) and a double-precision hybrid fast Hankel transform filter by Anderson (1989). The image method (dotted curve) uses the approximation formulas developed for a VMD by Bannister (1987; Table 2), and as modified for a layered earth via the Q-factor correction developed by Anderson (1991).

The image method and numerical integration method in Figure 1 depart significantly from each other at lower frequency for this example, but the HFS Q-method agrees much better with numerical integration at all frequencies in the chosen range. Note that the image method neglects certain wave guide modes as discussed by Anderson (1991), and therefore, it should not be expected to yield as good a result as with the other two methods.

Figure 2 shows another forward curve comparison with model parameters somewhat opposite than that used in Figure 1. In Figure 2, the agreement between the new HFS Q-method and numerical integration is still maintained as in Figure 1, whereas the image method, again, is only a rough approximation to the other methods. The oscillations above 30 MHz ( $3 \times 10^7$

Hz) in Figure 2 for all curves show some of the difficulties caused by a relatively thick second layer having a large dielectric contrast with the other layers. In this case, the integration solution should be used after 30 MHz. However, the present HFS system only samples up to about 24 MHz, and therefore, the HFS Q-method would still be a useful approximation here.

Figure 3 shows a completely different kind of model than in Figures 1 and 2. Again, the image curves in Figure 3 indicate a large departure from the other solutions at lower frequencies when conduction currents dominate. However, as frequency increases beyond 1 MHz ( $1 \times 10^6$  Hz) all three methods show good agreement with each other.

Differences between numerical integration and the Q-factor methods manifest themselves more in low-induction (i.e., quasi-static) problems than in the preceding examples. This can be illustrated by a 2-layer model having a very resistive basement as in Figure 4(b), where the low-frequencies were reduced down to 100 Hz and plotted as absolute ellipticity on a logarithmic scale to emphasize small numerical differences. In Figure 4(b) all curves depart significantly below about 300 kHz ( $3 \times 10^5$  Hz), which is near the first large peak in the image method tilt angle curve in Figure 4(a). Fortunately, for the current HFS system, results for all three methods converge better in the 300 kHz - 30 MHz range, as shown by the linear-log plots in Figures 4(c) and (d).

Extending the frequencies beyond 50 MHz into the gigahertz range is not anticipated for the present or future HFS hardware. But to show what would happen if that were attempted, a half-space example with the loops on the surface is given in Figure 5. For a half-space, equation (7) has  $\gamma_1^* = \gamma_1$ , and therefore equations (1)-(3) are exact solutions for all frequencies. In Figure 5, both the image and HFS Q-methods converge correctly up to 5 GHz ( $5 \times 10^9$  Hz). However, the numerical integration and Hankel transform digital filter obviously begins to break down at about 100 MHz ( $1 \times 10^8$  Hz). Thus, for this example, the HFS Q-method gives superior accuracy over numerical integration at all frequencies, and especially in the extreme gigahertz range.

For more examples and a detailed discussion on the range of validity of the Q-factor method to approximate layered model solutions, refer to Wait (1962) and Kraichman (1976).

## Discussion

Use of the new Q-factor method in inversion of HFS data is where significant improvements in computer time is realized over direct numerical integration inversion programs. In fact, the new HFS Q-method is generally about 1-to-2 orders of magnitude faster than with numerical integration inversion.

The image inversion algorithm (Anderson, 1991) is not as accurate as the other methods, but is slightly faster than the HFS Q-method. This is because the HFS Q-method requires more complex terms to evaluate  $H_z$  in equation (1) and  $H_r$  in equation (2) than in Bannister's (1987) simplified image theory formulas.

Use of a VMD source in the HFS Q-method is adequate as long as the  $r$ -separation is at least 5-times the transmitter loop diameter. If the VMD transmitter and receiver loops are above the surface, then without loss of generality, an additional air layer can be placed above the actual air-earth interface by using appropriate free-space constants ( $\sigma_0$ ,  $\mu_0$ ,  $\epsilon_0$ ).

### Conclusions

A new method for rapid computation of the EM field components for a VMD source on or above a layered earth has opened new doors for efficient inversion of HFS data. The method, called the HFS Q-method, is nearly as accurate as direct numerical integration, and in most cases, can replace the time-consuming interpretation studies previously reported by Stewart et al. (1994).

Many other classes of M-layer near-surface models were run to compare each of the three methods used in this report. In almost all cases, the new HFS Q-method showed acceptable agreement with the more exact numerical integration method in the 300 kHz to 30 MHz frequency range. Because of the accuracy and speed of the new HFS Q-method, the numerical integration method may not be needed to obtain a *final* least-squares fit to observed HFS data.

Hopefully, the HFS Q-method will become the method of choice for rapid interpretation of HFS data, and could easily be installed on a laptop PC for use while in the field.

### Acknowledgments

I especially wish to thank Dr. Mark Goldman, Institute for Petroleum Research and Geophysics, Israel, for his role in deriving the general solution (including displacement currents) for  $H_r$  and  $E_\phi$  in equations (2)-(3). Prior to his effort, only equation (1) was known to me as previously derived by Wait (1954).

The research described in this report has been jointly supported by the U.S. Department of Energy under contract # DE-AI07-92ID1320, and the U.S. Environmental Protection Agency, as noted below.

### Notice

Although the information in this document has been funded in part by the U.S. Environmental Protection Agency under interagency agreement DW-14933038-01-0 to the U.S. Geological Survey, it has not been subjected to Agency review. Therefore, it does not necessarily reflect the views of the Agency. The U.S. Government has the right to retain a non-exclusive royalty-free license in and to any copyright covering this article.

## References

- Anderson, W.L., 1989, A hybrid fast Hankel transform algorithm for electromagnetic modeling: *Geophysics*, **54**, 263-266.
- , 1991, Approximate inversion of high-frequency electromagnetic soundings using complex image theory: *Geophysics*, **56**, 1087-1092.
- Bannister, P.R., 1987, Extension of finitely conducting earth-image-theory results to any range, *in* Simplified expressions for the electromagnetic fields of elevated, surface, or buried dipole antennas: Naval Underwater Systems Center. (Also available as Navy Underwater Systems Center, Rep. 6885, 1984.)
- Kraichman, M.B., 1976, Handbook of electromagnetic propagation in conducting media: U.S. Government Printing Office, Stock No. 008-040-00074-5 (Library of Congress Catalog No. 77-609679), also available from Headquarters Naval Material Command Rept. NAVMAT P-2302.
- Ryu, J., Morrison, H.F., and Ward, S.H., 1970, Electromagnetic fields about a loop source of current: *Geophysics*, **35**, 862-896.
- Smith, B.D., and Ward, S.H., 1974, On the computation of polarization ellipse parameters: *Geophysics*, **39**, 867-869.
- Stewart, D.C., 1993, Detection of shallow subsurface layers by high-frequency sounding, PhD Thesis T-4374, Colorado School of Mines, 142 p.
- Stewart, D.C., Anderson, W.L., Grover, T.P., and Labson, V.F., 1994, Shallow subsurface mapping by electromagnetic sounding in the 300 kHz to 30 MHz range--Model studies and prototype system assessment: *Geophysics* [in press].
- Wait, J.R., 1954, Mutual coupling of loops lying on the ground: *Geophysics*, **19**, 290-296.
- , 1962, Electromagnetic waves in stratified media: The MacMillan Co., New York, N.Y., 372 p.

Figure 1 (a)

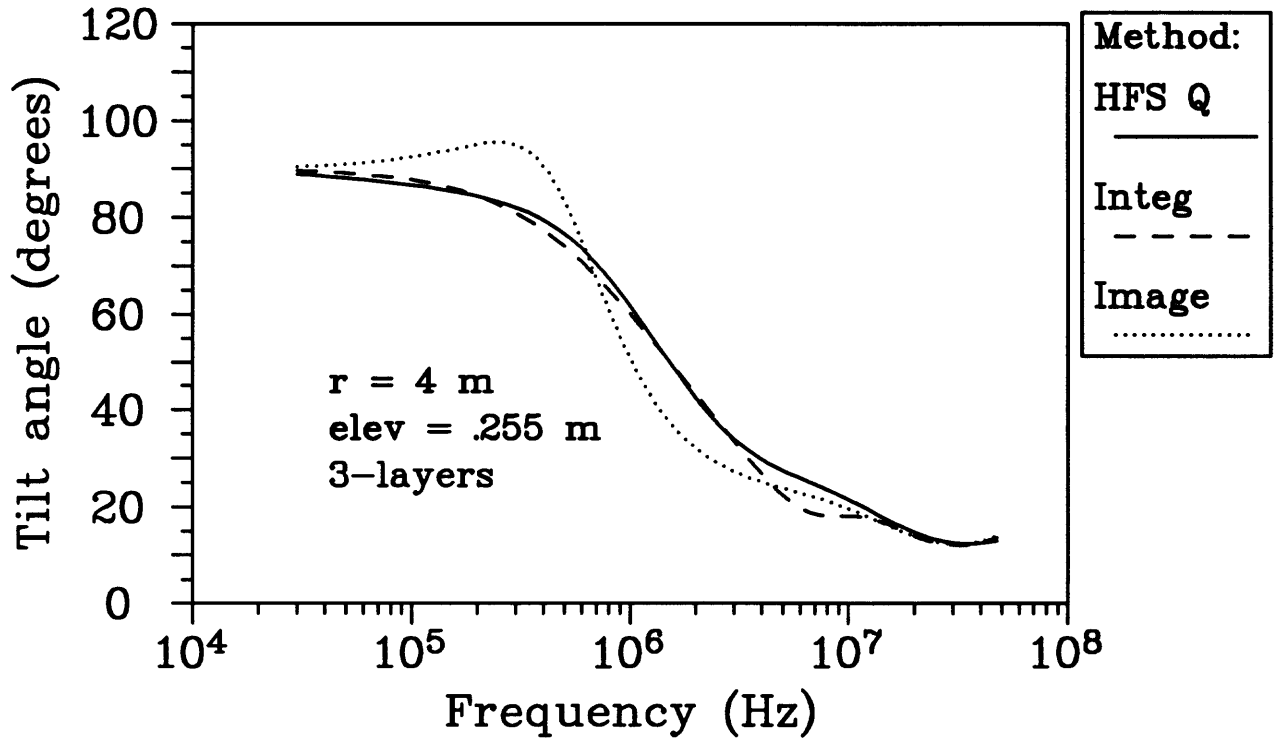


Figure 1 (b)

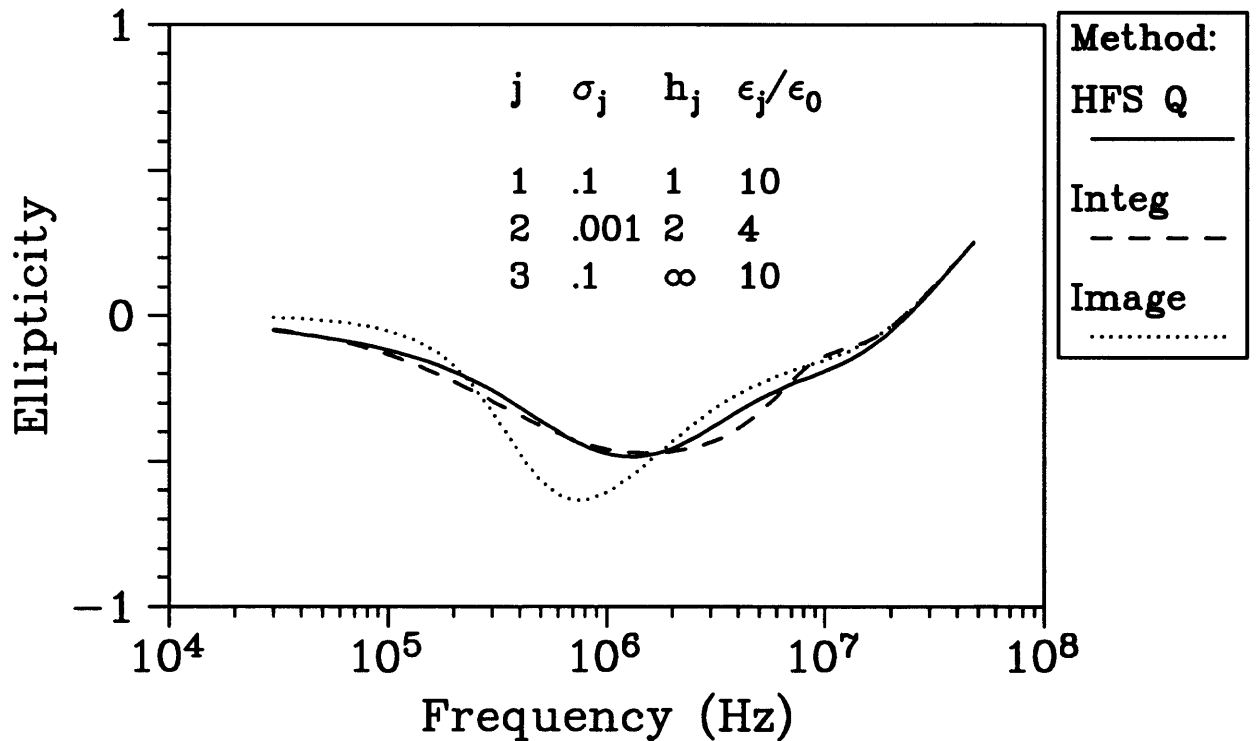




Figure 2 (a)

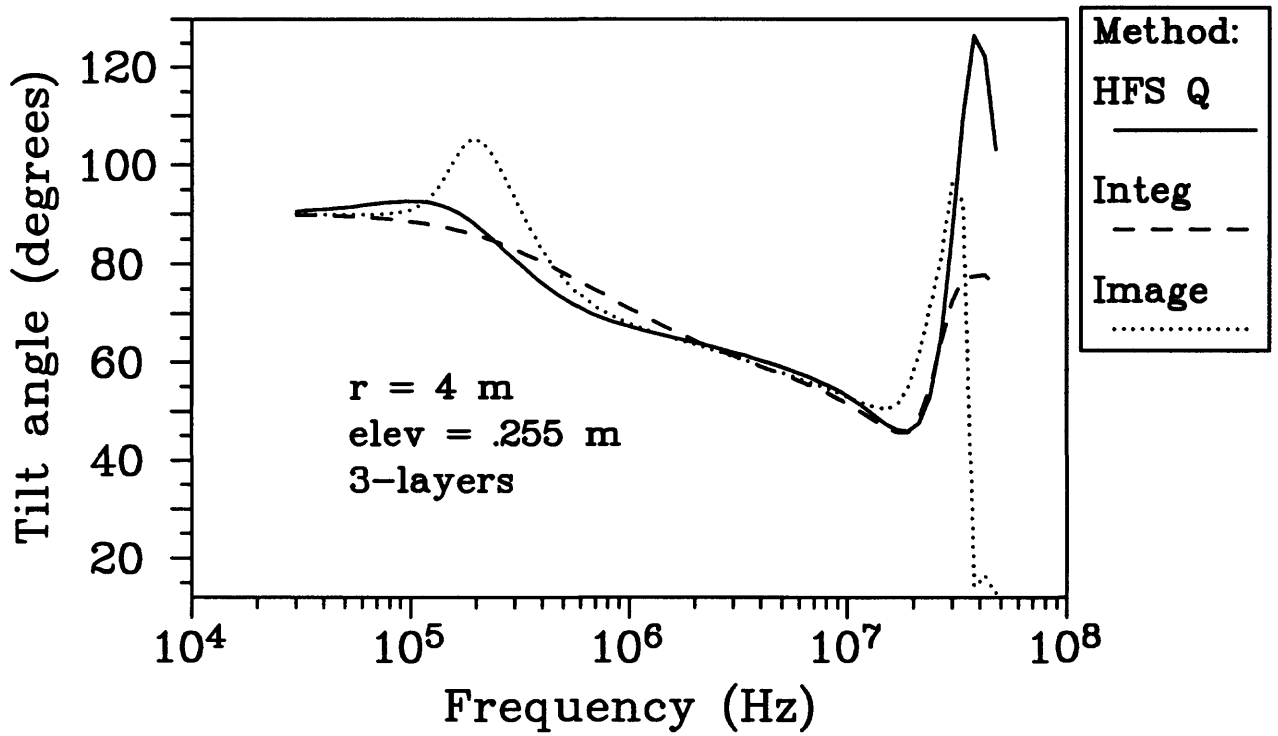


Figure 2 (b)

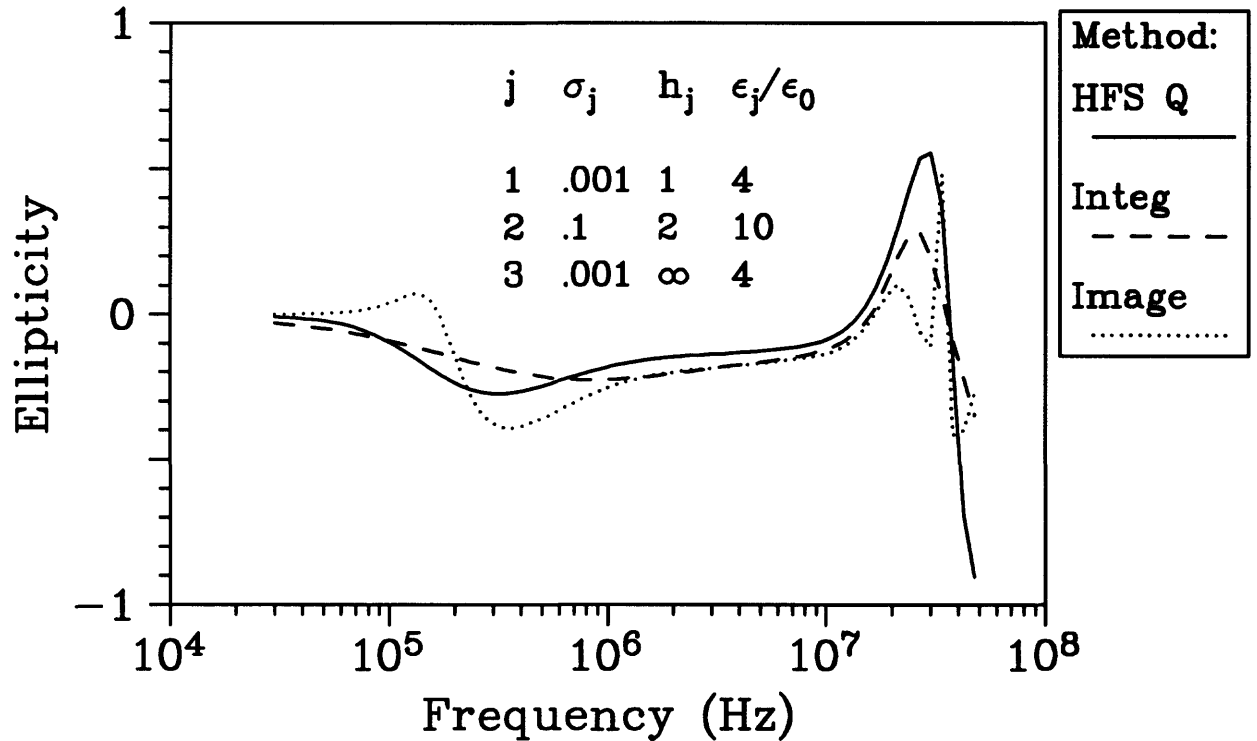


Figure 3 (a)

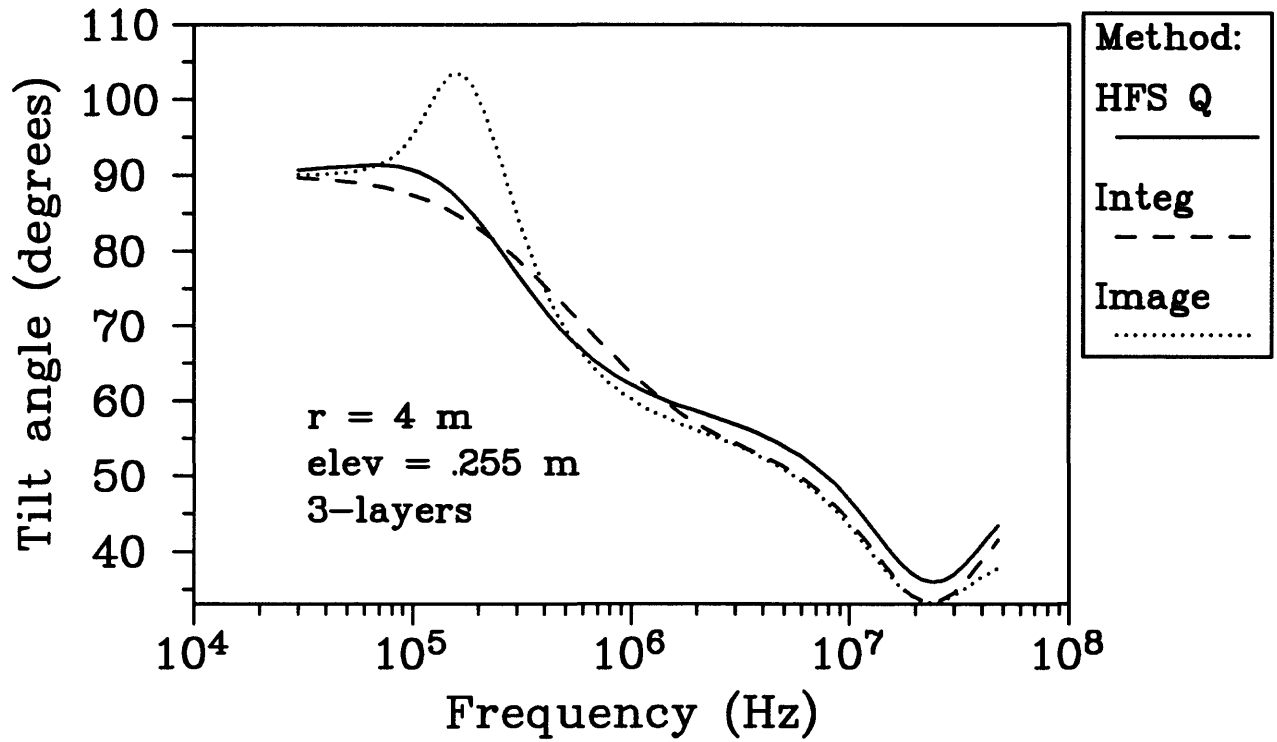


Figure 3 (b)

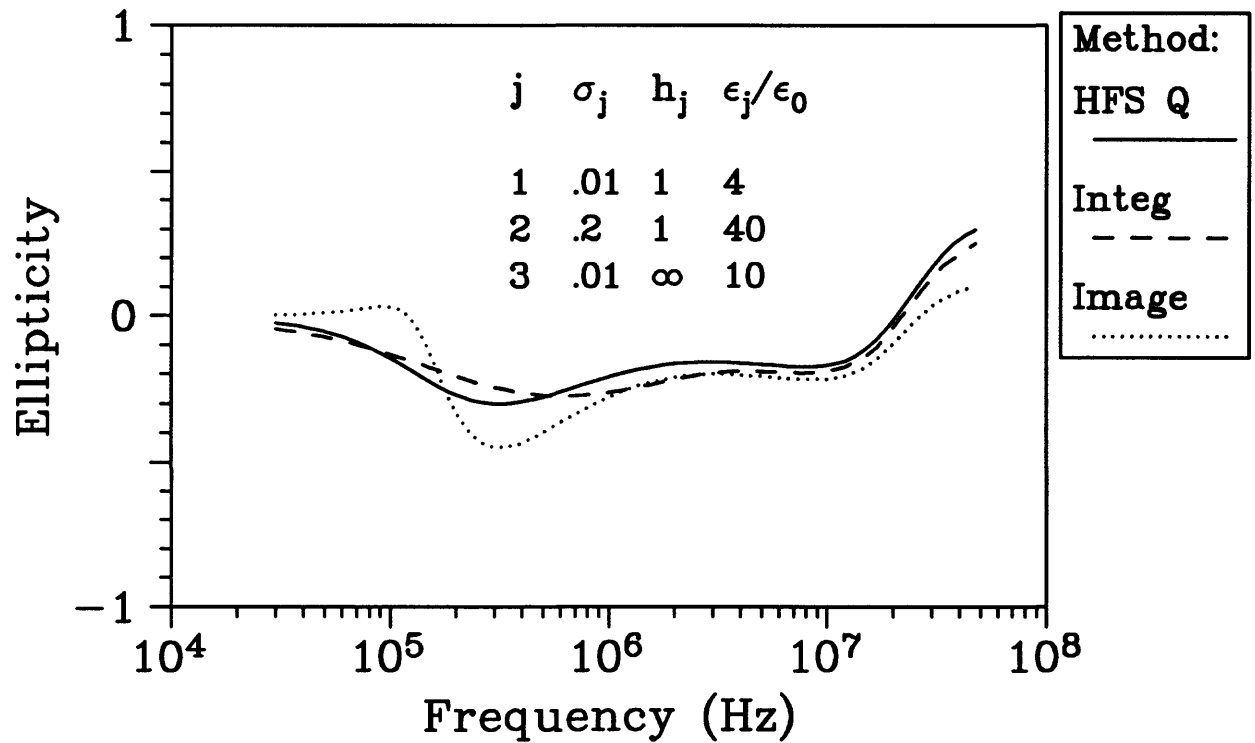


Figure 4 (a)

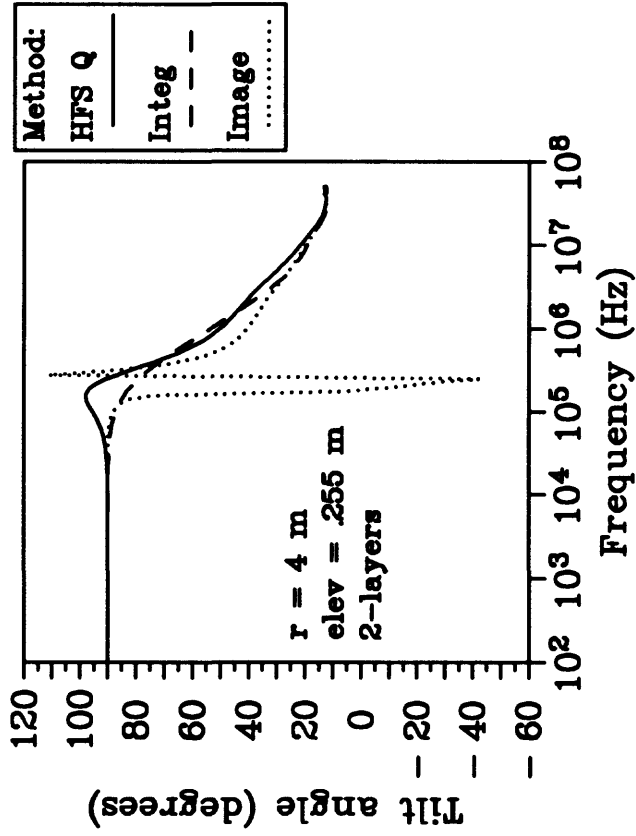


Figure 4 (b)

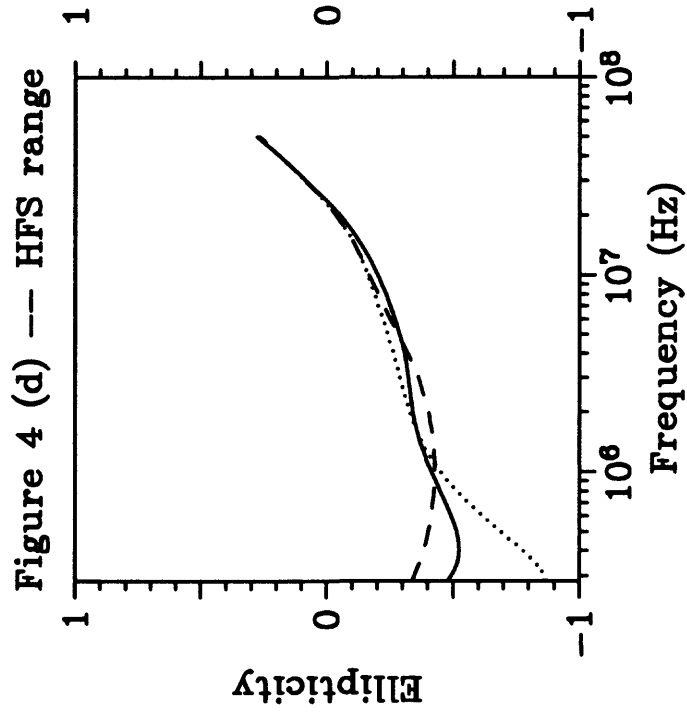
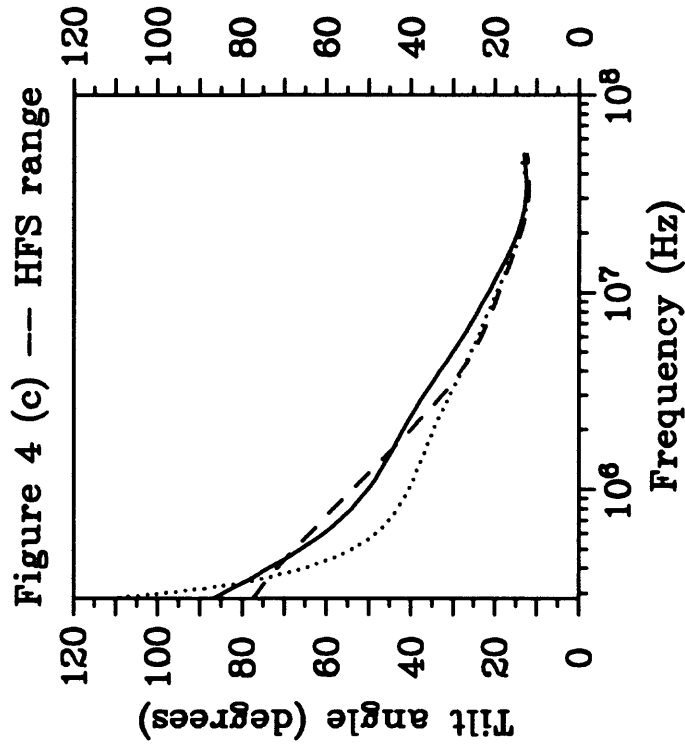
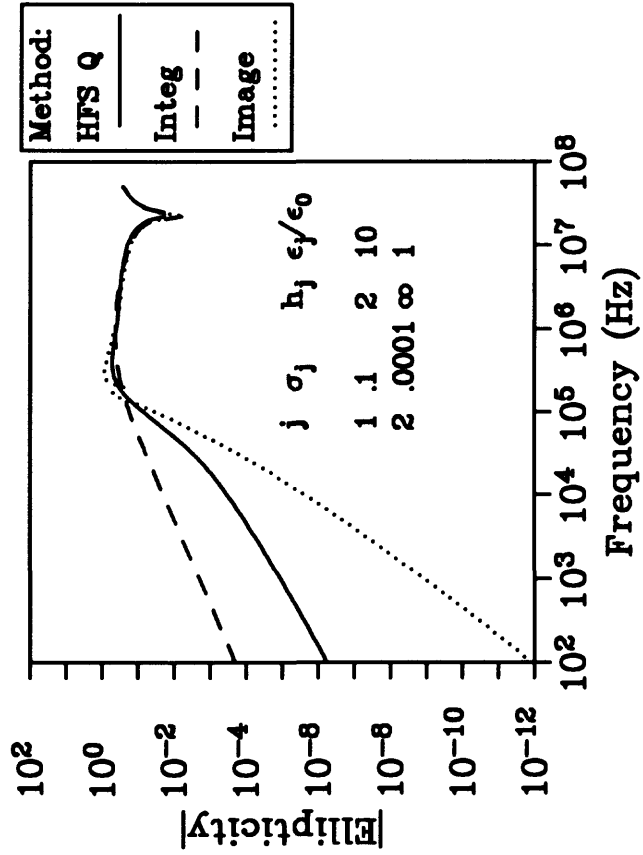


Figure 4 (a)–(d)

Figure 5 (a)

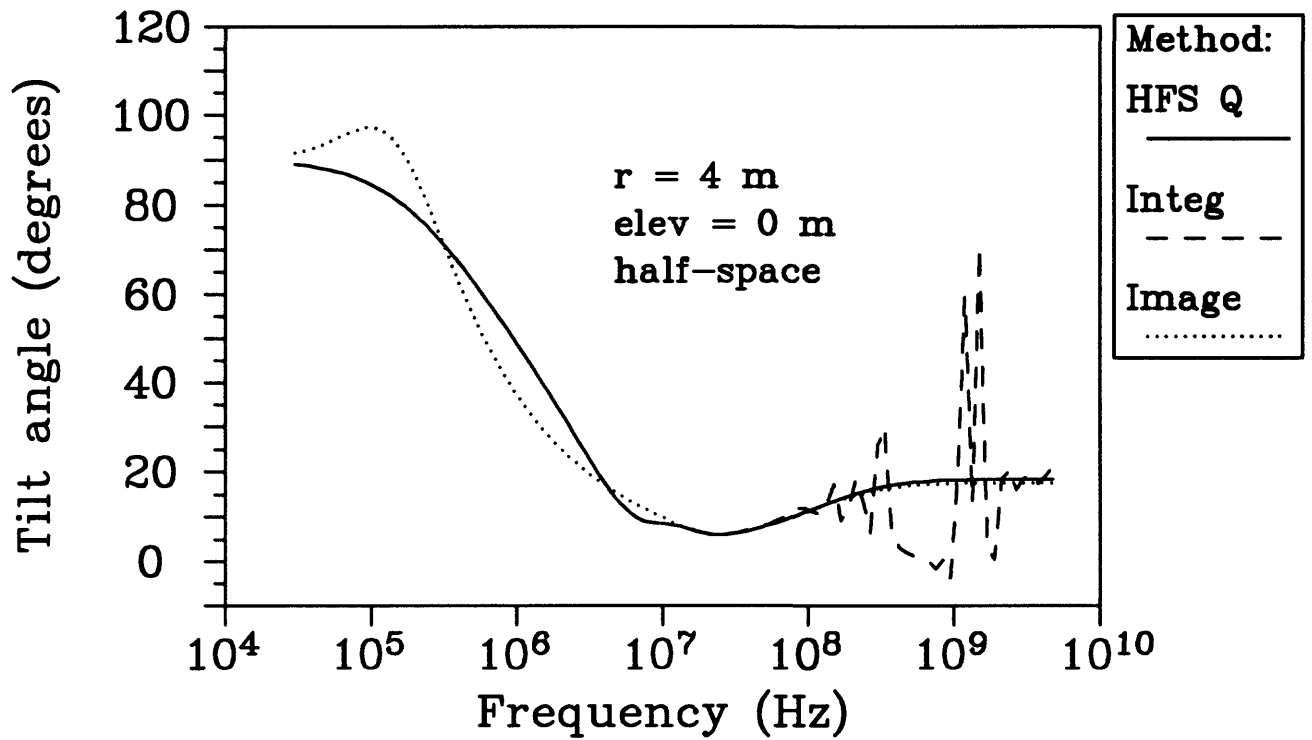


Figure 5 (b)

